

Shock tube studies on the formation of soot from the combustion and pyrolysis of some hydrocarbons

Margaret Evans and Alan Williams

Department of Fuel and Energy, The University of Leeds, Leeds LS2 9JT, UK

(Received 9 February 1981; revised 15 June 1981)

An investigation has been undertaken using a reflected shock tube to examine the formation of soot from toluene, benzene and straight-chain heptane. The properties of the soot formed depend on temperature, pressure and the concentration of the hydrocarbon being oxidized or pyrolysed. The reflected shock temperature of the gas was determined by measurements of the reflected pressure and the velocity of the incident shock wave. Samples of soot formed during the reaction were taken from the shock tube and examined using a transmission electron microscope to characterize the particles. Stereopairs were taken to determine their three-dimensional structure. The relative concentrations and type of soot produced were correlated with the reflected temperatures and information derived on the formation of the soot.

The formation of soot during the combustion of hydrocarbons is one of the major, as yet unsolved, problems of combustion chemistry. Although the basic features are well understood in relation to the nature of the products and with regard to the effect of different types of hydrocarbons, the detailed chemistry and nature of the soot produced are, as yet, not fully known. Soot, however, is known to be largely a carbonaceous material containing a small mass percentage of hydrogen as well as smaller amounts of oxygen in polycyclic compounds. A detailed understanding of all the steps of formation, prediction of yields and the nature of the products are also of great importance in relation to air pollution problems, the production of carbon black, radiant heat transfer process in flames, and gasification of aromatic-containing oil feedstocks.

Much work has been carried out in the field of carbon black. The structure and manufacture of carbon blacks have been reviewed by Donnet and Voet¹, the basic chemistry of soot formation in both aliphatic and aromatic compounds has been reviewed by Wagner² in a detailed analysis of the subject, and other reviews^{3,4} summarize the main features of carbon-producing systems and give information on the nature of carbon formation and the basic structures of the products formed. Very little, however, is known about the intermediate steps, the initial stages of soot production and the controlling factors. An attempt has been made by Coats and Williams⁵ in a recent paper to model the formation of soot in one simple case, that of straight-chain heptane during oxidation and pyrolysis. They modelled particle growth using the model proposed by Jensen⁶ for aliphatic compounds. In his model, C_2 , C_3 and C_2H were treated as initial nuclei for soot formation and acetylene was an intermediate species playing a major role in the soot production and particle growth. Each collision between an acetylene molecule and a soot particle was assumed to result in a combination forming a larger particle. For aromatic compounds it has been conclusively shown by Graham *et al.*⁷, using a shock tube, that there is an

alternative aromatic route involving dehydrogenation and ring fusion where the aromatic ring plays an important role. For both aliphatic and aromatic compounds, the carbon produced should have characteristic features which show up at both the early and later stages.

These investigations give some insight into the initial stages of soot production but neither have been paralleled by an experimental study of the actual types of soot produced. In this paper, a shock tube technique was used to sample soot produced in the reflected shock waves from both aliphatic and aromatic compounds, and the soot was studied by electron microscopy at early and later stages of the growth. There is a significant amount of data on the soot produced and these are analysed at least in part by reference to firstly the model used by Coats and Williams⁵ based on straight-chain heptane pyrolysis, and secondly by a less developed but equivalent model based on the growth of the soot molecules from aromatic nuclei.

The combustion kinetics of soot formation are extremely complex and although ideally it would be desirable to achieve rate expressions to describe the rate of soot formation under a variety of experimental conditions, the exact way of quantifying the soot yield remains a severe difficulty. It is clear from the results presented and also from earlier work, that the nature of the soot obtained is very much a function of the hydrocarbon used and of the temperature. It may be that the 'structure' of the soot produced in a combustion process could be an important factor in its subsequent burn-out in a combustion chamber, or in the influence that it subsequently has in environmental pollution or atmospheric chemistry.

EXPERIMENTAL

A reflected shock tube which has been previously described by Coats⁸ was used for the experiments. The test gases were made up of ANLAR toluene, benzene or straight-chain heptane, containing 1 mol% hydrocarbon

and 99 mol% argon for the pyrolysis experiment, and 1 mol% mixture of hydrocarbon, oxygen and argon constituting equivalence ratios of 0.5, 1.0, 2.0 and 4.0 for combustion. The conventional definition of equivalence ratio is used as previously⁸. Helium was used as driver gas. About ten experimental runs were carried out with the gases at different pressures for each mixture. During each shock the reflected pressure was measured using a Kistler pressure transducer coupled to a transient recorder, and the velocity of the shock wave was measured by recording the time taken for the shock to travel between five electret films placed at 150 mm intervals from the end of the tube. From these measurements the reflected temperature of the shock wave was calculated as previously⁸.

Soot from each run was collected and analysed. Copper electron microscope grids, 3 mm diameter, $\approx 30 \mu\text{m}$ thick and 400 mesh per inch, were coated with a continuous formvar (polyvinyl formal) support film. To make the film more stable in the electron beam and reduce drifting, the grids were vacuum coated with a thin layer (5 to 10 nm) of carbon. The fine structure of the carbon layer possesses very low contrast and does not interfere with the soot structure, except for high-resolution work, where perforated formvar films were made by mixing the formvar solution with glycerol. Some of the soot particles will lie over these holes and can be examined without any interference of background structure.

Two different methods to collect the soot from the shock tube were used. The first method was to collect the soot inside the tube. Each grid was attached carefully just inside the tube wall, or to the end plate of the shock tube with a very small amount of adhesive tape to ensure that the grid did not stick out from the surface of the plate and

interfere with the shock wave. After the shock had taken place, the grid was removed from the end plate and stored for electron microscopy.

The second method was to collect the soot outside the shock tube. A stainless-steel sample chamber was fitted onto the end plate of the tube which could be independently evacuated. A hole was made in the centre of the end plate, having a diameter of $\approx 350 \mu\text{m}$. This hole was covered with a small piece of gold foil, $25 \mu\text{m}$ thick to fit flush with the inside surface of the end plate, and containing a pin-hole of $100 \mu\text{m}$ diameter for the soot to be sampled through. Inside the chamber, directly in front of the pin-hole, was a metal wheel which could be rotated about an axis parallel to the end plate. Electron microscope grids were attached at certain intervals around the circumference of the wheel, facing the pin-hole, and the wheel could be turned during the reaction to study the soot formed at different stages.

The shock tube was cleaned thoroughly between each experiment and a run was carried out having the test section filled with air with an electron microscope grid in position. This grid was examined to ensure that no soot was being carried over from one experiment to the next. Test gas pressures of 2.0 and 4.7 kPa and driver gas pressures ranging from 51.7 to 137.9 kPa were used. After shock-heating the gas sample, air was admitted into the shock tube slowly and the end plate was removed as quickly as possible to retrieve the grid for examination. For some of the high soot-producing runs, a formvar-coated grid was held above the end plate when it was being removed to collect a sample of the smoke that was emitted from the shock tube.

The electron microscope used was a Phillips EM 200

Table 1 Shock conditions for toluene combustion (1% toluene in argon)

Run number (equivalence ratio)	Reflected shock pressure P_5 (kPa)	Reflected shock temperature T_5 (K)	Nature of the soot (units nm)	
			Single spheres	Chains
			Mean diam.	Mean diam, Mean length
T1 (0.5)	40.5	693	None	None
T2 (0.5)	64.9	846	None	None
T3 (0.5)	146.9	1216	Few, 33	Few; 52, 200
T4 (0.5)	266.5	1596	Few, 53	Few; 53, 170
T5 (0.5)	46.6	1067	Few, 38	None
T6 (0.5)	54.7	1161	Few, 38	None
T7 (0.5)	63.8	1297	Few, 42	Few; 42, 210
T8 (0.5)	115.5	1714	Few, 46	Few; 46, 140
T9 (1)	109.4	1073	None	None
T10 (1)	91.2	975	None	None
T11 (1)	147.9	1246	None	None
T12 (1)	222.9	2475	None	None
T12 (1)	219.9	2420	Few, 41	None
T14 (2)	97.3	1007	None	None
T15 (2)	154.0	1295	Few, 22	Many; 22, 280
T16 (2)	161.1	1349	Many, 22	Few; 22, 80
T17 (2)	186.4	1468	Many, 18	Few; 18, 100
T18 (2)	61.8	1253	Many, 25	Few; 25, 150
T19 (2)	84.1	1481	Few, 19	None
T20 (2)	173.3	2213	Few, 18	None
T21 (2)	158.1	2139	Few, 25	None
T22 (4)	92.2	1000	Many, ~ 100	None
T23 (4)	93.2	1012	None	None
T24 (4)	141.9	1319	None	Many; 20, 2500
T25 (4)	214.8	1641	Few, 18	Many; 18, 670
T26 (4)	64.9	1311	Few, 40	Many; 23, 700
T27 (4)	107.4	1685	Few, 31	Many; 20, 620
T28 (4)	166.2	2176	Few, 23	Many; 22, 320
T29 (4)	199.6	2453	Many, 46	Few; 46, 180

Table 2 Shock conditions for benzene combustion (1% benzene in argon)

Run number (equivalence ratio)	Reflected shock pressure P_5 (kPa)	Reflected shock temperature T_5 (K)	Nature of the soot (units nm)	
			Single spheres	Chains
			Mean diam.	Mean diam, Mean length
B1 (0.5)	80.0	937	None	None
B2 (0.5)	70.9	956	None	None
B3 (0.5)	63.8	888	None	None
B4 (0.5)	106.4	1149	Few, 27	None
B5 (0.5)	91.2	1090	Few, 19	None
B6 (0.5)	91.2	1102	Few, 35	None
B7 (0.5)	111.5	1742	Very few, 9	None
B8 (0.5)	82.1	1494	Very few, 20	None
B9 (0.5)	96.3	1685	Very few, 20	None
B10 (0.5)	118.6	1871	Very few, 23	None
B11 (0.5)	146.9	2061	Very few, 30	None
B12 (0.5)	154.0	2169	Very few, 40	None
B13 (1)	45.6	772	None	None
B14 (1)	63.8	947	None	None
B15 (1)	77.0	1050	None	None
B16 (1)	124.6	1244	None	None
B17 (1)	86.1	1099	None	None
B18 (1)	95.3	1147	None	None
B19 (1)	51.7	1344	Very few, 27	None
B20 (1)	61.8	1551	None	None
B21 (1)	106.4	1883	Few, 25	None
B22 (1)	107.4	1904	None	None
B23 (2)	57.8	890	None	None
B24 (2)	78.0	981	None	None
B25 (2)	67.9	973	None	Few; 29, 480
B26 (2)	83.1	1083	None	Many; 19, 500
B27 (2)	85.1	1123	Few, 28	Few; 27, 240
B28 (2)	96.3	1191	Few, 20	Few; 20, 140
B29 (2)	160.1	1464	Few, 26	Few; 26, 290
B30 (2)	47.6	1293	Few, 24	Few; 24, 95
B31 (2)	55.7	1432	Few, 21	None
B32 (2)	99.3	1826	Few, 20	None
B33 (2)	121.6	2051	Few, 20	None
B34 (2)	133.8	2160	None	None
B35 (4)	58.8	913	None	None
B36 (4)	122.6	1190	None	Many; 16, intertwined
B37 (4)	69.9	1008	Many, 45	None
B38 (4)	86.1	1273	None	Many; 14, ~2500
B39 (4)	93.2	1143	None	Many; 23, 250
B40 (4)	95.2	1199	None	Many; 14, intertwined
B41 (4)	69.9	1545	Few, 14	Many; 14, ~1500
B42 (4)	89.2	1662	Few, 17	Many; 17, 1000
B43 (4)	154.0	2300	Few, 19	Many; 19, 400
B44 (4)	122.6	2085	Few, 16	Small; 16, 350
B45 (4)	131.7	2185	Few, 19	Small; 19, 360

which is a conventional transmission electron microscope. Each sample was studied at a magnification of ≈ 6000 so that a general view of the particles could be seen and photographed for sizing. Higher magnification micrographs were taken to obtain a more detailed structural view of the individual particles. The micrographs of each sample were compared and size measurements made using a Quantimet 720 or a travelling microscope.

RESULTS

The experimental results are divided into four sections dealing with (a) toluene combustion, (b) benzene combustion, (c) straight-chain heptane combustion, and (d) pyrolysis. The reflected shock conditions for these categories and the structures and sizes of the soot collected from these runs are given in *Tables 1–4*, in the order of increasing temperature. The shocked gas

conditions were calculated from the initial test-gas pressure, the reflected shock pressure and the measured incident shock velocity using a computer programme⁸.

The soot samples collected were classified as simple spheres (particles) or chains (aggregates). The diameters of the individual spheres and the spheres linking up to make chains collected on one grid varied considerably. When a large amount of soot was produced many of the chains were lying on top of each other thus making it impossible to distinguish individual chains and hence their lengths could not be measured. The relative concentrations of soots produced were calculated from the photomicrographs on an area basis, using a Quantimet 720; i.e., the relative area of the grid covered by the soot gives an indication of the relative amount of soot present in the shocked gases.

Figures 1–13 show a selection of the micrographs taken showing particular features. *Figures 1–5* show the changes in the soot structure as the reflected shock temperature

Table 3 Shock conditions for straight-chain heptane combustion (1% heptane in argon)

Run number (equivalence ratio)	Reflected shock pressure P_5 (kPa)	Reflected shock temperature T_5 (K)	Nature of the soot (units nm)	
			Single spheres	Chains
			Mean diam.	Mean diam, Mean length
H1 (0.5)	69.9	843	Few, 15	None
H2 (0.5)	74.0	870	Few, 15	None
H3 (0.5)	98.3	951	Few, 28	None
H4 (0.5)	151.0	1116	Few, 50	None
H5 (0.5)	183.4	1203	Few, 50	None
H6 (0.5)	35.5	889	Few, 13	None
H7 (0.5)	51.7	1074	Many, 9	None
H8 (0.5)	94.2	1359	Very few, 12	None
H9 (0.5)	121.6	1495	None	None
H10 (0.5)	117.5	1496	Few, 16	None
H11 (0.5)	131.7	1609	Few, 37	None
H12 (1)	117.5	986	None	None
H13 (1)	172.3	1170	None	None
H14 (1)	191.5	1271	None	Few, 30, 150
H15 (1)	211.8	1358	None	None
H16 (1)	87.1	1289	None	None
H17 (1)	115.5	1495	None	None
H18 (1)	160.1	1798	Few, 40	Few, 25, 70
H19 (1)	146.9	1673	Very few, 25	None
H20 (2)	102.4	934	None	None
H21 (2)	156.1	1153	None	None
H22 (2)	197.6	1331	None	None
H23 (2)	219.9	1404	None	None
H24 (2)	115.5	1552	None	None
H25 (2)	121.6	1594	None	None
H26 (2)	161.6	1873	None	None
H27 (2)	157.1	1838	Few, 25	None
H28 (4)	114.5	991	None	None
H29 (4)	128.7	1044	None	None
H30 (4)	223.9	1372	None	None
H31 (4)	242.2	1425	None	None
H32 (4)	279.7	1544	None	None
H33 (4)	237.1	1426	None	None
H34 (4)	276.6	1545	Few, 25	None
H35 (4)	174.3	1895	Few, 44	None
H36 (4)	208.7	2127	Few, 19	Few; 19, 75
H37 (4)	266.5	2454	Few, 19	Few; 19, 60

increases from 1000 K to 2300 K during typical rich combustion runs (B37 to B45) for benzene with $\phi = 4$, and Figures 6–9 show the changes with increase in temperature during pyrolysis (runs P3 to P8) using toluene. When less soot was formed, as with the leaner mixtures, the pattern of soot formation followed that shown in Figures 10–13 for the combustion of toluene with $\phi = 2$. During some runs with weak mixtures a few spheres were formed at ≈ 1000 K. Figure 12 is a high magnification micrograph, showing the fine structure of particles formed during the pyrolysis of toluene (P4).

Stereopairs were taken of some of the soot particles in order to see the three-dimensional structure. For stereopair production⁹, the first micrograph was taken at -6° to the electron beam and the second micrograph was taken at $+6^\circ$, making sure that the magnification and field of view were the same to avoid eyestrain and distortion, and that the contrast of the micrographs were similar. Figure 13 shows a stereopair taken of the soot from run P4. In order to view the stereopair correctly¹⁰, any parallax created by tilting the sample in the microscope must be parallel to the line of viewing. As the parallax exists in a direction perpendicular to the tilt axis, the tilt axis must be perpendicular to the line of viewing of the stereopairs. The stereopairs taken with the Phillips EM 200 microscope must be rotated through 90° to fulfil

the above requirement. When viewed with a stereoviewer, Figure 13 exhibits a three-dimensional structure from which the heights of different particles can be measured.

Some soot emission measurements were made using a monochromator and photomultiplier at 615 nm. The results obtained for straight-chain heptane and benzene undergoing combustion are given in Figure 14. The relative soot yields measured from the three fuels under pyrolysis conditions are plotted in Figure 15 and under combustion conditions for $\phi = 2$ and 4 in Figure 16. The soot yields for leaner mixtures were very low. Thus for toluene at $\phi = 0.5$ the maximum yield on the same scale as Figure 16 was 0.53 at 1297 K, and at $\phi = 1$ it was 3.9 at 1295 K. With benzene and heptane the yields were even smaller, being less than 0.2.

DISCUSSION

Nature of soot formation

In general, as is to be expected, toluene and benzene produced higher soot yields than straight-chain heptane. The soot that was formed in the shock tube consisted of either single spheres (particles) or spheres joining up to make chains (aggregates). The type and amount of soot formed was found to be related to the reflected shock

Table 4 Shock conditions for toluene, benzene and straight-chain heptane pyrolysis (1% in argon)

Run number (hydrocarbon)	Reflected shock pressure P_5 (kPa)	Reflected shock temperature T_5 (K)	Nature of the soot (units nm)	
			Single spheres	Chains
			Mean diam.	Mean diam, Mean length
P1 (toluene)	39.5	715	None	None
P2 (toluene)	83.1	976	None	None
P3 (toluene)	120.6	1107	Many, 70	None
P4 (toluene)	145.9	1332	None	Many; 19, 4000
P5 (toluene)	40.5	1193	Few, 24	Jagged; 24, 460
P6 (toluene)	47.6	1217	None	Many; 18, 5000
P7 (toluene)	74.0	1509	Few, 29	Many; 29, 4000
P8 (toluene)	154.0	2159	Few, 25	Many; 25, 2000
P9 (benzene)	74.0	1012	None	None
P10 (benzene)	89.2	1115	None	None
P11 (benzene)	71.9	1039	Hazy, 44	None
P12 (benzene)	79.0	1098	None	Many; 26, 2500
P13 (benzene)	87.1	1154	None	Many; 24, intertwined
P14 (benzene)	119.6	1323	None	Many; 24, intertwined
P15 (benzene)	50.7	1369	None	None
P16 (benzene)	81.1	1735	Few, 22	Few; 22, 1500
P17 (benzene)	68.9	1668	None	None
P18 (benzene)	100.3	1924	Few, 22	Many; 22, 950
P19 (benzene)	177.3	2588	Few, 23	Many; 23, 900
P20 (n-heptane)	53.7	776	None	None
P21 (n-heptane)	108.4	1018	None	None
P22 (n-heptane)	92.2	971	None	None
P23 (n-heptane)	115.5	1086	None	None
P24 (n-heptane)	151.0	1196	Many, 44	None
P25 (n-heptane)	158.1	1245	Few, 26	Few; 23, 360
P26 (n-heptane)	87.1	1410	Few, 24	None
P27 (n-heptane)	55.7	1202	Few, 21	None
P28 (n-heptane)	94.2	1501	Many, 37	Few; 37, 90
P29 (n-heptane)	106.4	1623	Few, 25	Many; 25, 500

temperature. The appearance of soot forming at low temperatures, at ≈ 1000 K, varied with the equivalence ratio of the hydrocarbon. When the mixture was rich (equivalence ratio 4) or during pyrolysis the low-temperature soot consisted of single particles, each surrounded by a greasy-looking haze as shown in *Figures 1* and *6*. As the temperature is low when this haze is formed, it could be incompletely burned fuel depositing on the shock tube walls, or it may be an intermediate species, i.e. a soot precursor, as illustrated in the low-temperature route to soot described later. At ≈ 1100 – 1200 K this haze began to disappear (*Figures 2* and *7*), and very jagged chains formed which were made up of spheres ≈ 24 nm diameter. Above this temperature long chains were formed which were made up of smaller spheres ≈ 16 nm diameter (*Figures 3* and *8*). These chains broke down to smaller chains at higher temperatures. The break down occurred faster during rich combustion runs than during pyrolysis runs (*Figures 4*, *5* and *9*). The amount of soot produced during combustion of rich mixtures and pyrolysis increased as the temperature increased up to a maximum at ≈ 1300 K. Above this temperature the amount of soot decreased and often at temperatures at ≈ 2400 K there were only a few spheres produced.

The hydrogen mixtures with equivalence ratios of 2, 1 and 0.5 produced less soot than the rich mixtures, again as expected. The pattern of soot formation generally followed that shown in *Figures 10* and *11*. With this mixture (toluene, equivalence ratio 2) at 1000 K no soot was formed but in general with the weaker mixtures single spheres were formed at ≈ 1000 K followed by a few small chains at 1200 K to 1300 K (*Figure 10*). These broke down

slowly to give simple spheres at ≈ 2000 K (*Figure 11*). In this sequence the maximum amount of soot formed was at 1295 K (*Figure 10*), where the chains were longest and most numerous.

The relative concentration of soot was measured using the Quantimet 720. The area of soot particles on each grid was calculated for each sample. At low concentrations the area could be easily assessed but at higher concentrations, as in *Figure 8*, there would be particles on top of each other and the concentration would be an underestimate. However, the results given in *Figures 15* and *16* show that with increasing temperature there is an increase in concentration up to a maximum level and then a decrease in concentration for each mixture tested.

The internal structure of the soot particles was not studied in detail. *Figure 12* shows some structure but the magnification and resolution are not sufficiently high to determine the full nature of this structure, although the short lines visible in the particles could be the constituent lamellar molecules of the carbon black. This soot sample had only reached a temperature of 1332 K but soot samples that had been above 2000 K were studied in the same way and showed similar structures. It has been shown by Crawford *et al.*¹¹, who studied soot from a detonation wave, that although soot produced in this way has reached a sufficiently high temperature for graphitization to take place, the residence time at this temperature was inadequate to graphitize the soot particles. Hence, they have the appearance of a low-temperature carbon (≈ 1200 K) rather than having ordered, stacked crystallites as in a graphitized sample.

In *Figure 13*, the maximum height from the top to the

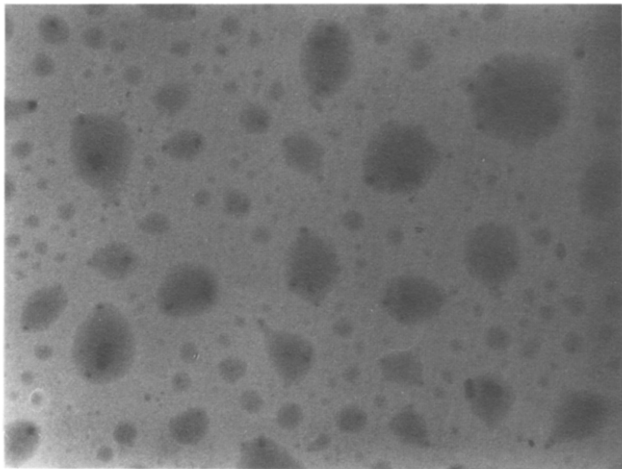


Figure 1

500 nm

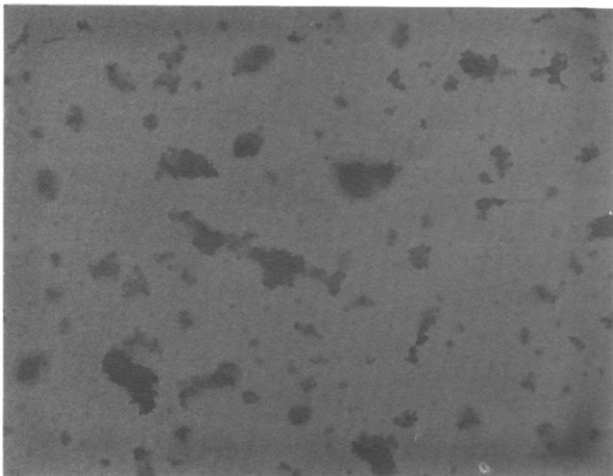


Figure 2

500nm

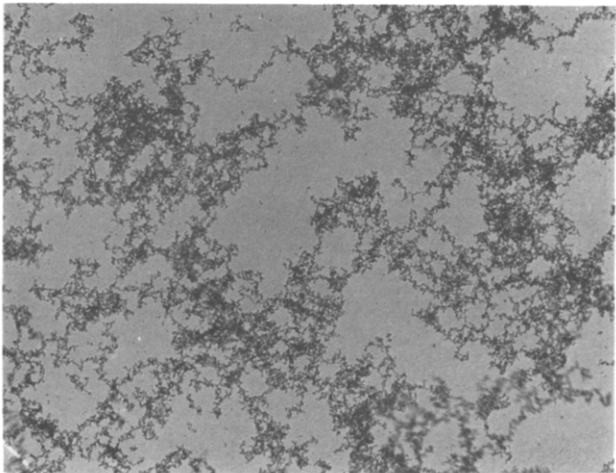


Figure 3

500nm

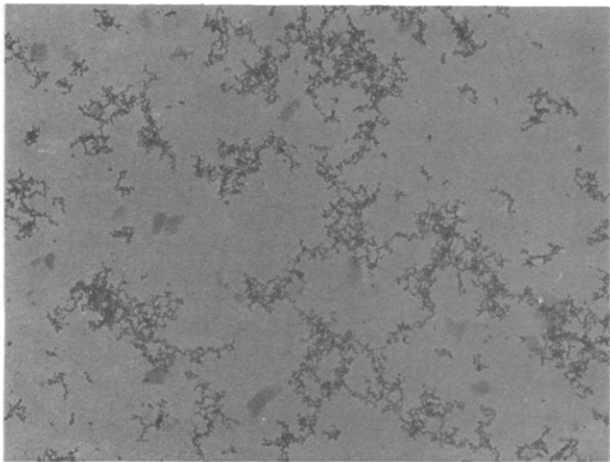


Figure 4

500nm

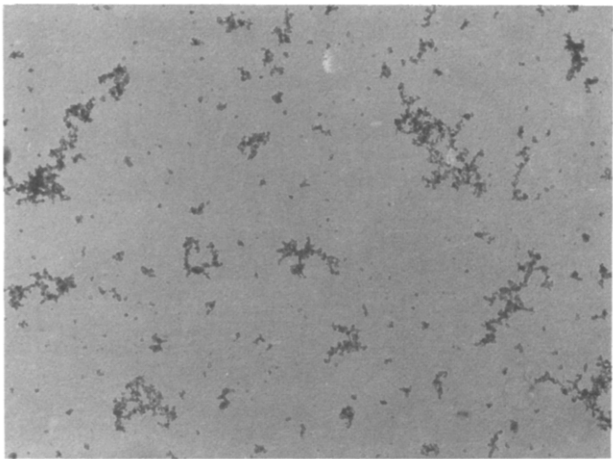


Figure 5

500nm

Figures 1–5 Transmission electron micrographs of soot from shock tube combustion of benzene, equivalence ratio 4, run numbers B36 to B43. T_s is the reflected temperature. T_s : Figure 1, 1008 K; Figure 2, 1143 K; Figure 3, 1273 K; Figure 4, 1545 K; Figure 5, 2300 K

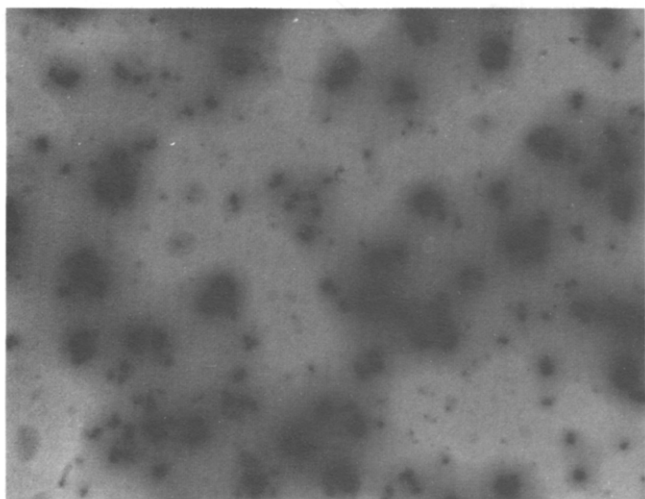


Figure 6

500 nm

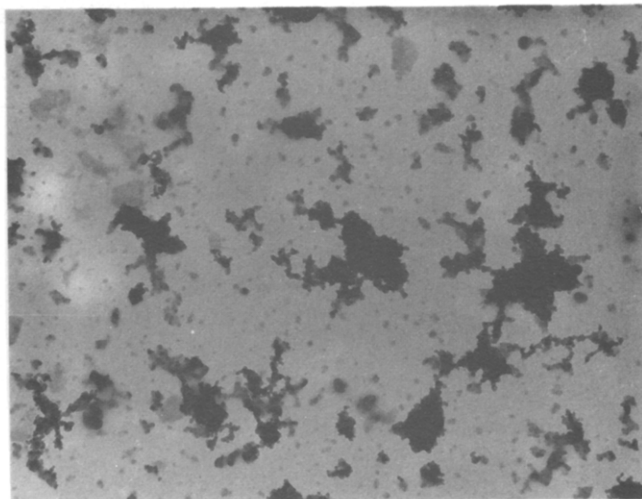


Figure 7

500 nm

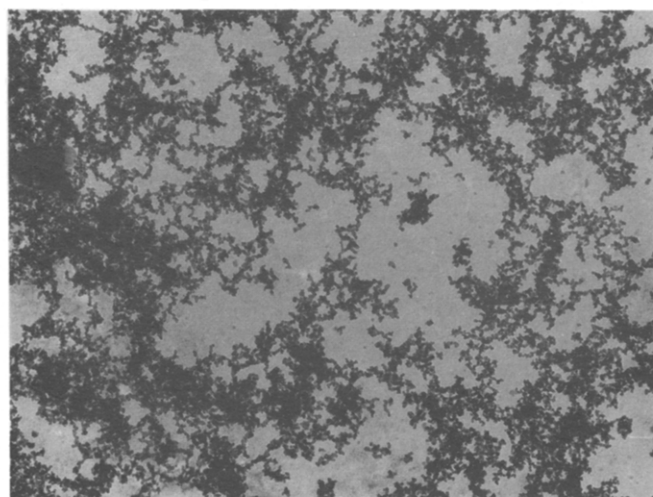


Figure 8

500 nm

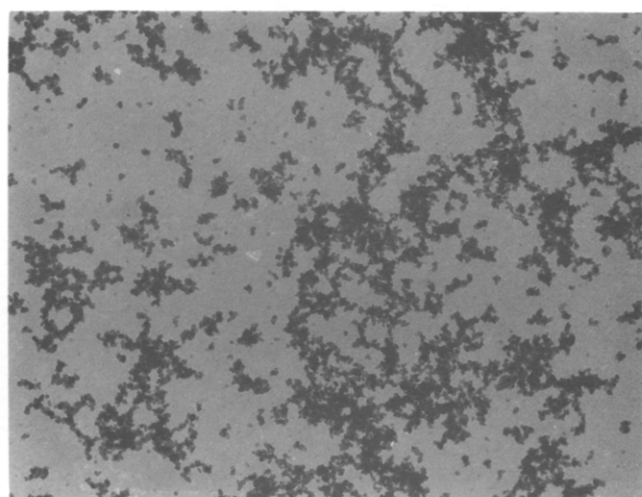


Figure 9

500 nm

Figures 6–9 Transmission electron micrographs of soot from shock tube pyrolysis of toluene, run numbers P3 to P8. T_s is the reflected temperature. T_s : Figure 6, 1107 K; Figure 7, 1193 K; Figure 8, 1332 K; Figure 9, 2195 K

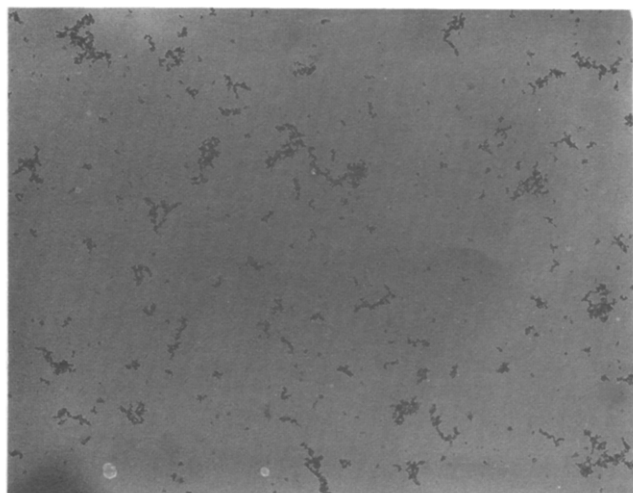


Figure 10

500 nm

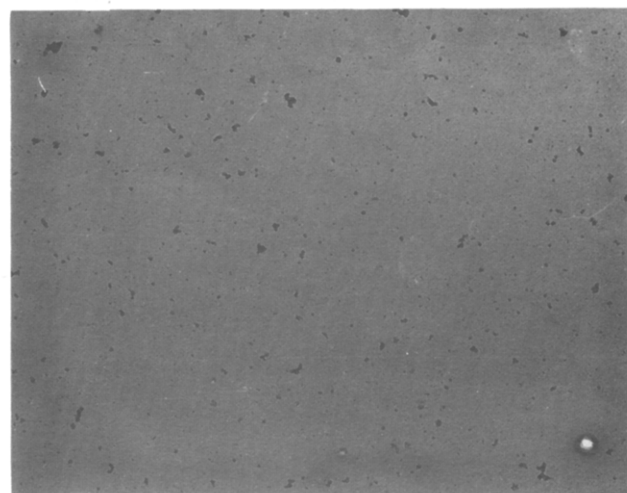


Figure 11

500 nm

Figures 10 and 11 Transmission electron micrographs of soot from shock tube combustion of toluene, equivalence ratio 2, run numbers T15 to T21. T_s is the reflected temperature. T_s : Figure 10, 1295 K; Figure 11, 1468 K

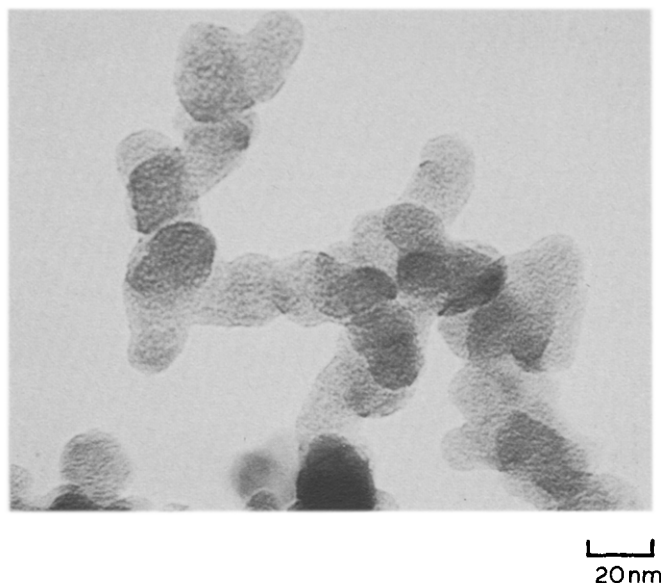


Figure 12 Transmission electron micrograph of soot from shock tube pyrolysis of toluene, run number P4. Reflected temperature 1332 K

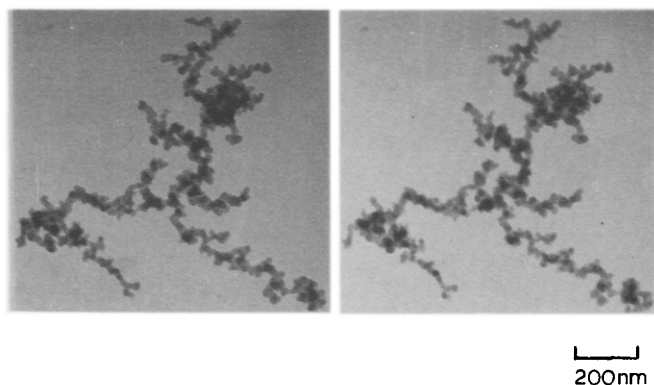


Figure 13 Stereopair of soot from shock tube pyrolysis of toluene, run number P4. Reflected temperature 1332 K

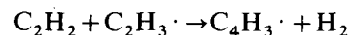
bottom of the soot aggregate, calculated by measuring the stereoscopic parallax¹² on the micrographs, was ≈ 100 nm. From this stereopair, coordinates of one point with respect to others can be calculated using stereoscopic plotting instruments giving their relative positions within the three-dimensional image. Mercer *et al.*¹³ have made solid models of carbon black aggregates from electron stereomicrographs. They used a mirror stereoscope and plotted out many points around the surface of the image. The solid model enabled the 'image' to be held and viewed from any direction.

Mechanism of soot formation

A recent review⁴ of carbon black formation shows that although a great deal of work has been carried out on soot formation and different mechanisms have been proposed, the exact mechanism by which soot is formed during the combustion of hydrocarbons has not yet been fully established.

There is now substantial evidence to suggest that during the pyrolysis or combustion of rich mixtures of aliphatic hydrocarbons, acetylene and polyacetylenic species play an important role in soot formation. Polyaromatic compounds are also present but their

formation occurs after the formation of the polyacetylenes. Homann and Wagner¹⁴ suggested that nucleation starts with acetylene combining to form a straight-chain radical as follows:



This, in turn, produces diacetylene which combines with

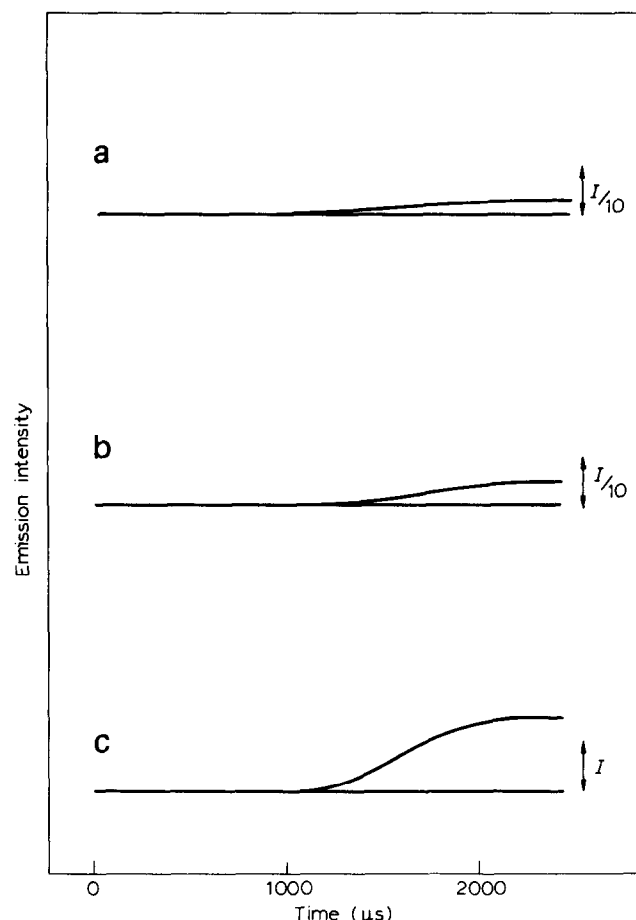


Figure 14 Soot emission during combustion at 615 nm for (a) straight-chain heptane; $\phi = 4$; $T = 1545$ K (run H34); (b) straight-chain heptane; $\phi = 4$; $T = 2127$ K (run H36); and (c) benzene; $\phi = 4$; $T = 1545$ K (run B41)

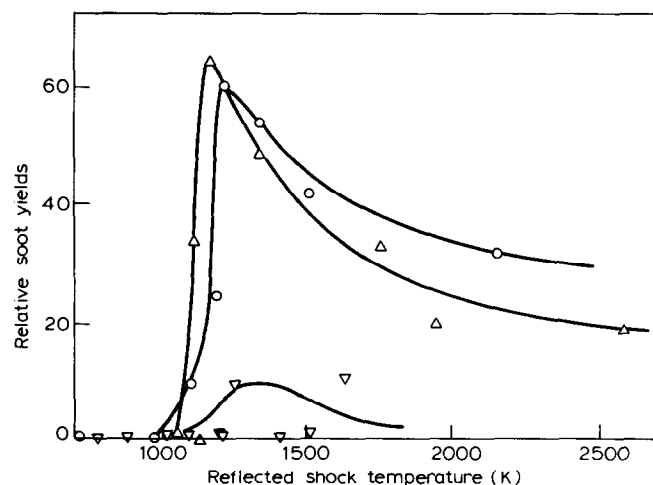


Figure 15 Variation of relative soot concentration with temperature during the pyrolysis of Δ , benzene; \circ , toluene; and ∇ , straight-chain heptane

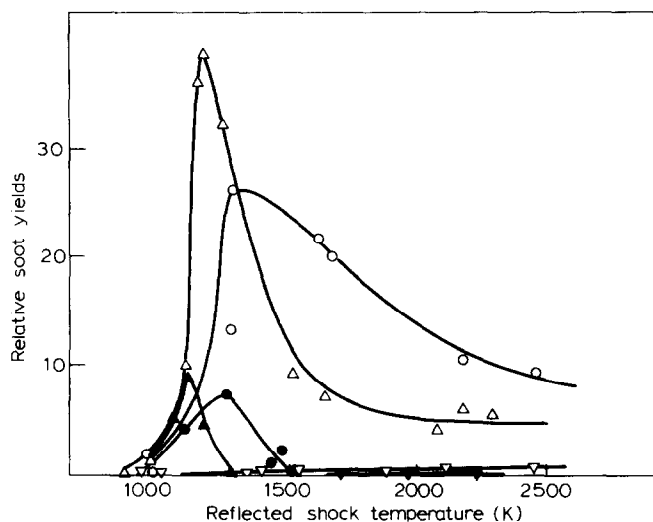
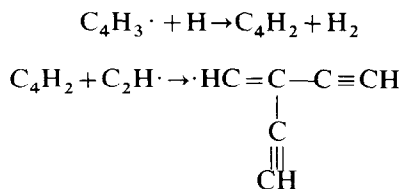


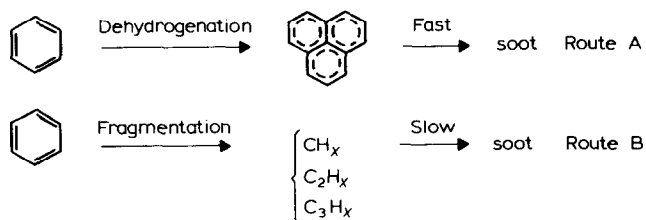
Figure 16 Variation of the relative soot concentration with temperature during the oxidation with $\phi = 4$ for Δ , benzene; \circ , toluene; and ∇ , straight-chain heptane; and $\phi = 2$ for \blacktriangle , benzene; \bullet , toluene; and \blacktriangledown , straight-chain heptane

an ethynyl radical to produce the first soot species:-



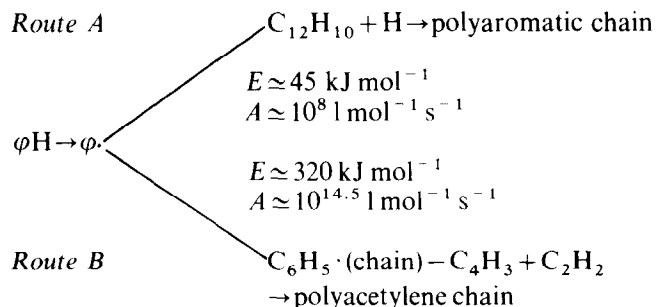
These polyacetylene radicals then combine with further polyacetylenes to produce large branched radicals. Thus, the first phase in carbon formation is the nucleation of a particle. Once an initial nucleus is formed the particle growth rate increases rapidly with small particles readily combining to form larger ones. This has been demonstrated previously by a computer model developed in this laboratory⁵.

In the pyrolysis of aromatic compounds, other routes become available as shown, for example, by Graham *et al.*⁷. They studied soot yields from aromatic hydrocarbons using a shock tube in the temperature range 1600–2300 K and found that the soot yield at 2300 K was twenty-fold less than the yield at 1750–1800 K. They suggested that this was due to a competition being established between a slow and a fast route from the hydrocarbon to the production of soot. These two routes are illustrated by the overall reactions:



The first route involving dehydrogenation and ring fusion is an efficient low-temperature direct route which gives way at higher temperatures to the second less efficient indirect route involving ring fission, soot being the ultimate product of both routes. The fall in yield with increasing temperature indicates that the second reaction becomes more effective but it is a slower indirect route and

takes longer to reach completion. This becomes clear from the kinetics of the alternative initial steps, for example, for benzene:



The kinetic data is taken from the estimates given by Asaba and Fujii¹⁵. Clearly, route A is preferred at low temperatures because of its low activation energy (E) of 45 kJ mol⁻¹; at high temperatures route B is preferred although it has a higher activation energy, because the pre-exponential factor (A) is also higher and has first-order kinetics. Thus a gradual switch from A to B occurs with increase in temperature but, at least using the mechanism suggested here, it seems that route A must always dominate over route B. Presumably the maximum soot yield obtained is a consequence of reverse reactions, or depolymerization coming into dominance. A similar situation would apply to toluene, although the initial radical would be $\phi\text{CH}_2\cdot$, the individual steps would be basically the same with condensation being balanced against ring fission and decomposition.

This interpretation would account for our results for both toluene and benzene. Figure 15 shows the variation of soot concentration with reflected temperature for the pyrolysis of toluene, benzene and straight-chain heptane. For toluene and benzene the soot yield starts off at zero at ≈ 1000 K, increases to 60% at 1200 K and then decreases to 20% at ≈ 2200 K. During combustion the trend was very similar although soot yields were less, especially with the weak mixtures. The soot yield during the pyrolysis of straight-chain heptane (Figure 15) did not follow the same trend but showed a maximum soot yield at a temperature of 1450 K. The yield for straight-chain heptane was six times less than that for toluene and benzene. It is highly probable that aliphatic hydrocarbons would produce soot mainly via the indirect slow route (B), breaking down to acetylene and forming radical species such as $\text{C}_4\text{H}_3\cdot$ and $\text{C}_6\text{H}_3\cdot$ as previously discussed. Therefore the soot yield is much lower than for aromatic hydrocarbons, with benzene producing slightly more soot and maximizing at a lower temperature than toluene.

Structurally there is little information to be obtained about the immediate soot precursor. At low temperatures the indistinct 'greasy' material is obtained which cannot be defined as soot. The smallest well-defined soot particles are in the 11–40 nm diameter range, as shown in Figure 12. An 11 nm diameter particle would contain $\approx 7.5 \times 10^4$ carbon atoms whereas the individual lamellae (Figure 12) have dimensions of ≈ 2 nm. These would correspond to carbon particles of about C_{100} and are consistent with the suggestion of Wang *et al.*¹⁶ that the important soot precursor is circumcoronene, $\text{C}_{96}\text{H}_{24}$.

Figure 16 shows the variation of the relative soot concentrations with temperature during the oxidation of benzene, toluene and straight-chain heptane with $\phi = 4$. The shapes of the curves are similar to those exhibited for

pyrolysis (Figure 15), with toluene giving the highest yield but this being at a lower temperature than for benzene. However, in this oxidative situation the yield from straight-chain heptane is virtually zero, in contrast to the results from pyrolysis (*cf.* Figure 15). It is seen, as might be expected, that even in pyrolysis the yields from straight-chain heptane are much smaller than for the aromatic compounds studied and the maximum yield occurs at a higher temperature.

Soot emission measurements made at 615 nm are shown in Figure 14. The three different intensity curves correspond to different types of soot formed. Figure 14a corresponds to spheres formed with a haze around them giving a low intensity. Figure 14b corresponds to the formation of spheres and very small chains and Figure 14c corresponds to the formation of a large amount of soot with many long chains present. At low temperatures where no soot was formed, the emission trace was along the base line. This is consistent with the data given in Figure 16. Details of the rates of soot formation deduced from this work will be published in a future paper.

CONCLUSIONS

(1) At low temperatures (below 1000 K) a greasy haze is visible around the soot particles on the electron microscope grids. This could be due to incomplete combustion, leaving very small droplets of fuel condensing onto the shock tube walls.

(2) Combustion and pyrolysis of the aromatic hydrocarbons followed two paths to produce soot. One was a low temperature fast efficient route which gave way at higher temperatures to the other which was a slow inefficient route. This caused the maximum amount of soot to be produced at about 1300 K when the second route became effective. As the concentration of soot increased, the chain length also increased and as the concentration decreased, the chains became smaller until single spheres were present.

(3) Combustion and pyrolysis of the aliphatic hydrocarbon appeared to produce soot in the following way: (a) Formation of radical species $C_4H_3\cdot$ and $C_6H_3\cdot$; (b) Formation of polyacetylenes from these species; (c) Formation of soot nuclei by the addition of hydrocarbon radicals to polyacetylenes; and (d) Particle growth by the building up and addition of acetylene molecules. This route corresponds to the second stage in the slow

inefficient reaction of aromatic hydrocarbons to produce soot.

(4) Electron microscopy has been a useful technique for studying physically the type, size and concentration of soot produced in a shock tube and for monitoring the build up of soot particles to produce very long winding chains.

ACKNOWLEDGEMENTS

The authors are grateful to the British Gas Corporation for a Fellowship (to Margaret Evans), the Science Research Council for a research grant for equipment and technical support, and Lucas CAV for a gift of a laser.

REFERENCES

- 1 Donnet, J. B. and Voet, A. 'Carbon Black' Marcel Dekker Inc., New York, 1976
- 2 Wagner, H. G. G. Soot Formation in Combustion, 17th Symposium on Combustion, The Combustion Institute, 1978, p. 3
- 3 Palmer, H. B. and Cullis, C. F. 'The Formation of Carbon from Gases, Chemistry and Physics of Carbon' (Ed. Walker, P. L., Jr.) 1965, Vol. 1, p. 265
- 4 Lahaye, J. and Prado, G. 'Mechanisms of Carbon Black Formation, Chemistry and Physics of Carbon' (Ed. Walker, P. L., Jr.) 1978, Vol. 14, p. 167
- 5 Coats, C. M. and Williams, A. Investigation of the Ignition and Combustion of n-Heptane-Oxygen Mixtures, 17th Symposium on Combustion, The Combustion Institute, 1978, p. 611
- 6 Jensen, D. E. *Proc. Roy. Soc.* 1974, **A338**, 375
- 7 Graham, S. C., Homer, J. B. and Rosenfeld, J. L. J. *Proc. Roy. Soc.* 1975, **A344**, 259
- 8 Coats, C. M. *Ph.D. Thesis* The University of Leeds, 1978
- 9 Wells, O. C. 'Scanning Electron Microscopy' McGraw Hill, New York, 1974
- 10 Hearle, J. W. S., Sparrow, J. T. and Cross, P. M. 'The Use of the S.E.M.' *Ch.* 11, 1971
- 11 Crawford, D., Marsh, H. and Ubbelohde, A. R. A Phase-Contrast High-Resolution Electron Microscope Study of Carbon Flocs. 5th London International Carbon and Graphite Conference, 1978, p. 12
- 12 Boyde, A. *J. of Microscopy* 1973, **98**, 452
- 13 Mercer, H. N., Boyer, A. H., Brusky, P. L. and Deviney, M. L. *Rubber Chem. Tech.* 1976, **49** (4), 1068
- 14 Homann, K. H. and Wagner, H. G. G. *Proc. Roy. Soc.* 1968, **A307**, 141
- 15 Asaba, T. and Fujii, N. Shock-Tube Study of High Temperature Pyrolysis of Benzene, 13th International Symposium on Combustion, The Combustion Institute, Pittsburgh, 1972, p. 155
- 16 Wang, T. S., Matula, R. A. and Farmer, R. C. Combustion Kinetics of Soot Formation from Toluene, 18th Int. Symposium on Combustion, The Combustion Institute. To be published